Environmental Science & Technology

pubs.acs.org/est

Article

Sediment Ballet: Unveiling the Dynamics of Metal Bioavailability in Sediments Following Resuspension and Reequilibration

Dejin Xu,[§] Haiyan Xiong,[§] Qiuling Wu, Wenze Xiao, Stuart L. Simpson, Qiao-Guo Tan, Rong Chen, and Minwei Xie*

Cite This: https://doi.org/10.1021/acs.est.4c08327

Read Online

ACCESS | Metrics & More | Article Recommendations | Supporting Information

ABSTRACT: Assessing the risk of metal-contaminated sediments under disturbed conditions is challenging due to the lack of methods that capture instant changes in metal bioavailability. Existing approaches provide inadequate understandings of the processes regulating metal bioavailability under nonequilibrium conditions. Experiments were conducted to improve our understanding of the metal bioavailability dynamics induced by sediment resuspension and subsequent redeposition (reequilibration). An isotopically modified bioassay, a novel stable isotope tracing technique, was used to measure metal bioavailability (assimilation rates) to clams within short time windows. Changes in metal partitioning were characterized by porewater analysis using in situ extraction and the diffusive gradients in thin-films technique. Results showed that sediment resuspension released metals into porewater, while reequilibration scavenged metals from the porewater. The assimilation rates of Ni, Cu, and Pb increased with the resuspension time, aligning with increasing porewater concentrations. Unexpectedly, during reequilibration, the metal assimilation rates did not decrease. The discrepancies between bioavailability to the clam and porewater extrapolations may be due to differing sustained conditions of metals in sediments. Overall, this study unveils the metal bioavailability dynamics in nonequilibrium sediments, which could not be accurately predicted relying solely on porewater analysis. Incorporating rapid bioassays to determine bioavailability offers a valuable tool for robust ecological risk assessment.

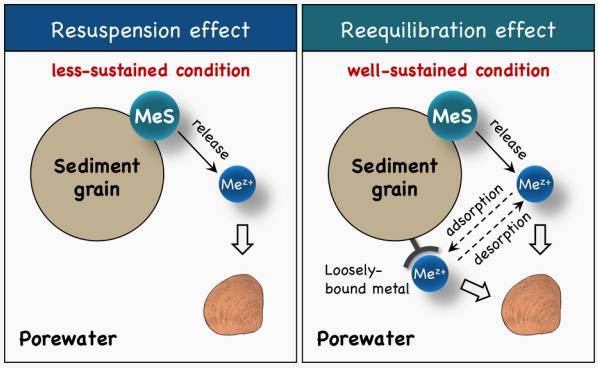

KEYWORDS: *metal pollution, oxidation, porewater partitioning, bioassay, nonequilibrium, toxicity risk assessment*

1. INTRODUCTION

Sediment resuspension, driven by natural events or anthropogenic activities, is an important pathway for transporting contaminated sediments[1,2] and exposing metal contaminants to aquatic organisms.[3] Studies have demonstrated that resuspended metal-contaminated sediments exhibit enhanced toxicity.[4−6] However, this is not reflected in standard risk assessment practices or current sediment quality guidelines,[7,8] which typically assume that porewater under equilibrium conditions represents the bioavailable metal exposure.[9−11]

Sediment resuspension and deposition represent common nonequilibrium conditions,[2] causing transitions between reducing and oxidizing conditions that alter the behavior of redox-sensitive contaminants.[12] In organic-rich, fine-grained sediments, metals primarily exist as metal sulfides,[9,13] which readily oxidize upon suspension in oxic conditions.[14−16] While the chemical transformation of metal species during resuspension[15−17] and redeposition[18−20] is well understood, gaps persist in understanding the processes regulating metal bioavailability,[21] challenging accurate environmental risk assessments.

Probing transient changes in metal bioavailability in disturbed sediments is challenging, especially under dynamic conditions requiring rapid bioavailability measurement.[21,22] Conventional biological approaches, such as long-term bioaccumulation methods and toxicity tests, directly assess metal bioavailability at the completion of tests[23,24] but fail to capture instant bioavailability changes.[25] More rapid chemical approaches, like acid-volatile sulfide extraction (AVS) and simultaneously extracted metal (SEM) measurements, extrapolate bioavailability based on the understanding of metal-sulfide biogeochemistry.[9] However, these indirect methods are better suited for predicting the absence of metal risks (e.g., when SEM < AVS), yet they are less effective in identifying the presence of risks (e.g., when SEM > AVS).[10]

Received: August 11, 2024
Revised: December 5, 2024
Accepted: December 5, 2024

In previous studies, we developed an isotopically modified bioassay to measure metal bioavailability within short time windows.[26−28] This technique, adapted from a "reverse-labeling" method,[29,30] measures metal bioavailability by tracing changes in isotopic composition in isotope-enriched organisms following exposure to bioavailable metals. The method has been successfully applied in sedimentary environments to directly measure the net influx rates of multiple metals, or "assimilation rates", which can be incorporated into kinetic models to predict bioaccumulation.[28] As the bioassay provides direct and rapid metal bioavailability measurements, it is well-suited for revealing dynamic changes in metal bioavailability influenced by sediment resuspension.

The primary objective of this study was to improve our understanding of the dynamics of metal bioavailability induced by sediment resuspension and the subsequent equilibration process. Experiments were conducted to (1) characterize chemical changes associated with metal partitioning during sediment resuspension and reequilibration, (2) examine the effect of sediment resuspension durations on dynamic changes in metal bioavailability, and (3) analyze changes in metal bioavailability during the reequilibration process.

2. MATERIALS AND METHODS

2.1. General Methods. All glassware and plasticware were cleaned by soaking in 5% HNO_3 for at least 12 h, rinsed with deionized water (18.2 MΩ cm, Millipore, USA) three times, and air-dried in a clean environment.

2.2. Sediment, Water, Organisms, and Metal Stable Isotopes. Contaminated sediment was collected in November 2021 from a tributary river in the Pearl River Estuary (22°45′2″ N, 113°46′10″ E), Shenzhen, Guangdong Province, China. The sediment, fine-grained and contaminated with Ni, Cu, Zn, Cd, and Pb,[27,31] was collected from the surface (depth <10 cm), transferred into a 20 L plastic bucket, sealed, and transported to the laboratory. The sediment was stored at room temperature (21 ± 1 °C) and used within six months.

Reconstituted freshwater was prepared by dissolving chemical salts in reverse osmosis (RO) water, with the composition per liter consisting of 62 mg $MgSO_4{\cdot}7H_2O$, 63 mg $CaSO_4{\cdot}2H_2O$, 96 mg $NaHCO_3$, 50 mg $CaCl_2$, and 4 mg KCl.[32] The freshwater was freshly prepared and aerated overnight before being used for organism culture and experimentation.

Asian clams (*Corbicula fluminea*) with shell lengths of 1.2−1.6 cm were collected from a clean river located in Guangdong (23°28′40″ N, 113°49′46″ E) and transported to the laboratory. Clams were acclimated for 1 week at laboratory conditions (21 ± 1 °C and natural light−dark cycle). During the acclimation period, clams were fed daily with green algae *Chlorella* sp. (3.5 mg clam^{-1}) for 1 h before water renewal.

Metal stable isotopes (^{62}Ni, ^{65}Cu, ^{68}Zn, ^{114}Cd, and ^{206}Pb) with purities >99% were purchased from ISOFLEX, USA.

2.3. Isotopically Modified Bioassay to Determine Metal Bioavailability in Sediments. The isotopically modified bioassay approach was employed to assess metal bioavailability in sediments, consisting of two stages: isotopic modification and sediment exposure.

2.3.1. Isotopic-Modification Stage. The goal of this stage is to increase the abundance of labeling isotopes within clam tissue. Clams were cultured in 10 L of reconstituted freshwater spiked with stable isotopes (5 μg L^{-1} ^{62}Ni, 10 μg L^{-1} ^{65}Cu, 10 μg L^{-1} ^{68}Zn, 3 μg L^{-1} ^{114}Cd, and 5 μg L^{-1} ^{206}Pb) for 7 days. A flow-through system maintained consistent isotope concentrations, renewing the spiked water concentration to 4.6 mL min^{-1}. Clams were fed daily as previously described in separate containers and rinsed before returning to the culture system.

To monitor isotopic composition changes, ten clams were sampled on the first, third, and seventh days. Clams were immersed in a 1 mM ethylenediaminetetraacetic acid (EDTA) solution for 1 min to terminate further isotope uptake and then dissected with a stainless-steel scalpel. Soft tissues were rinsed with EDTA and then with deionized water to remove surface contaminants and then stored at −20 °C for metal analysis.

2.3.2. Sediment Exposure Stage. Following the isotopic-modification stage, clams were exposed to sediments in the box-container setup (Section 2.4), with seven clams per box.

The clams were exposed to sediments for 10 h, informed by previous studies showing that 1 h was sufficient for assessing Cd bioavailability in suspended sediments[26] and 24 h suitable for Ni and Pb in equilibrated sediments.[27,28] Given the rapid changes in metal speciation during resuspension, this 10 h exposure can capture dynamic shifts in bioavailability while maintaining measurement sensitivity within the 168 h experiment.

After a 10 h sediment exposure, clams were removed from sediments, rinsed with RO water to remove attached particles, and transferred to clean reconstituted freshwater for a 12 h depuration to eliminate undigested sediments. Water was renewed when feces were observed. At the end of depuration, all clams were taken and processed following the aforementioned procedures (Section 2.3.1).

A reference group of isotopically modified clams not exposed to contaminated sediments served as a baseline for comparison. By comparing the isotopic composition of the test clams with the reference clams, we could quantify the assimilation of bioavailable metals from the sediment (Section 2.7).

2.4. Resuspension and Equilibration Experiments. The experiments were conducted in three runs (*Run1*, *Run2*, and *Run3*) to investigate the influence of sediment resuspension and the reequilibration on metal bioavailability. *Experiment Run1* focused on the chemical changes in metal partitioning between the dissolved and particulate phases during resuspension and reequilibration. *Experiment Run2* and *Run3* examined dynamic changes in metal bioavailability in sediments subjected to varying resuspension durations (*Run2*) and reequilibration periods (*Run3*), utilizing an isotopically modified bioassay to determine metal bioavailability.

2.4.1. Experiment Run1: Initial Chemical Characterization of Sediment Resuspension and Reequilibration. Sediment resuspension was performed in a 3 L glass conical flask by mixing 0.7 L of wet sediment with 0.7 L of reconstituted fresh water. The flask was placed on a reciprocating shaker at 210 ± 10 rpm and covered with aluminum foil (with pinholes) to prevent splashing and allow air exchange. The resuspension test was performed in triplicate and lasted for 7 days (168 h).

At designated intervals (5 min, 2 h, 12 h, 24 h, 72 h, and 168 h), sediment slurry samples were characterized by measuring dissolved oxygen concentration, pH, dissolved alkalinity, dissolved metal concentrations, AVS content, and SEM concentrations, as described in Note S2, Supporting Information.

Sediment reequilibration was conducted by placing 7 d resuspended sediments into small plastic boxes (7.5 cm length × 7.5 cm width × 5 cm depth) and equilibrating them in larger plastic containers (26 cm length × 16 cm width × 16 cm

https://doi.org/10.1021/acs.est.4c08327
Environ. Sci. Technol. XXXX, XXX, XXX−XXX

depth) under water for 2 to 336 h (2 weeks). Triplicate boxes were used for each equilibration interval. Each box contained sediment settled to a depth of 4 cm, with 4 L of overlying water added to the larger containers to submerge the sediments to a depth of 12 cm. Throughout the equilibration period, the water column was aerated through four aquarium stones to ensure the mixing.

At designated equilibration times (2, 12, 24, 72, 168, and 336 h), porewater chemistry was analyzed using passive samplers, specifically diffusive gradients in thin-films (DGT) devices (Section 2.5). For each time interval, the water in the larger plastic container was renewed, and a piston-type DGT sampler was deployed into the sediments for 10 h to measure labile metal concentrations.

Right before retrieving DGT samplers, porewater samples were also collected in situ using a microporous porewater sampler.[27] This sampler consists of a hollow fiber (5 cm long, 2 mm in diameter, and pore size of 0.15 μm) connected to a plastic syringe needle adapter and was preinstalled by inserting it horizontally 2 cm from the bottom of the small boxes.

2.4.2. Experiment Run2: Effect of Resuspension Duration on Metal Bioavailability. To investigate changes in metal bioavailability in redeposited sediments following different resuspension durations (2, 12, 24, 72, and 168 h), resuspension pretreatments were scheduled to align measurement times, minimizing potential variability in physiological conditions among organisms.

Prepared within the reequilibration box and container setup described in Section 2.4.1, triplicates of sediment from each resuspension interval were stabilized for 2 h to allow sediment settling. Subsequently, seven isotopically modified clams were added to each plastic box and exposed for 10 h to determine metal bioavailability (detailed in Section 2.3). Concurrently, a piston DGT sampler was deployed for 10 h to characterize the metal lability. Porewater was sampled at the end of organism sediment exposure.

2.4.3. Experiment Run3: Effect of Reequilibration Duration on Metal Bioavailability. To investigate the effect of sediment reequilibration on metal bioavailability, isotopically modified bioassays were conducted on sediments resuspended for 7 days and equilibrated for different durations (2, 12, 24, 72, and 168 h). Similar to the method used in *Experiment Run2*, the resuspension and equilibration pretreatments were prescheduled to ensure simultaneous exposure of organisms to the sediments.

Sediments were also prepared as previously described in the reequilibration box and container setup. Water in the larger containers was renewed before seven isotopically modified clams were introduced. In contrast to *Experiment Run1* and *Run2* that used piston DGT samplers, self-assembled planar DGT samplers (described in Section 2.5) were deployed to investigate labile metal depth profiles. Porewater was also sampled using the microporous sampler at the end of organism exposure.

2.5. DGT Application: Deployment of Piston and Planar DGT Samplers. DGT technique was used to measure labile metal concentrations in sediments. When deployed, the DGT devices accumulate metals from porewater, which diffuse through the membrane filter and gel layer before binding to the resin. The depletion of metals in porewater is then replenished by weakly bound metals from the sediments.[33] Therefore, the DGT devices capture labile metals from both porewater and sediment sources. For detailed operational procedures, refer to Note S1 in the Supporting Information. Below is a concise overview of the main procedures.

Two types of DGT samplers were used: planar DGT and piston DGT devices.[33,34] Prior to deployment, both types of DGT were deoxygenated by bubbling nitrogen gas in 0.05 M NaCl solution for at least 4 h. The piston DGTs, sourced from DGT Research Ltd., were inserted vertically to measure metal concentrations at depths of 0.5 to 2.5 cm (exposure area of 3.14 cm^2). The planar DGT, assembled in the laboratory, consisted of a membrane filter and two gel layers (also from DGT Research Ltd.) housed within a rectangular plastic holder with a measurement window of 2.5 cm width × 6 cm length. This sampler was inserted 3 cm into the sediment to measure the metal profiles across the sediment water interface. After a 10 h deployment, the samplers were retrieved, cleaned, and stored for analysis.

Within a month of retrieval, the metal-binding layer from piston DGT samplers was directly digested in 1 M HNO_3 solution. For planar DGT samplers, the metal-binding layer gel was sectioned into 5 mm slices within 2.5 cm of the sediment−water interface and then digested. The eluent was analyzed using ICP−MS for Mn, Fe, Ni, Pb, Cu, Zn, and Cd. The time-integrated average concentration of labile metals was then calculated.[35]

Blank DGT samplers, which underwent the same procedures without sediment deployment, accounted for background contamination. The measured concentrations in the deployed samplers were substantially higher than the background metal concentrations and were corrected by subtracting the mean blank concentrations.

2.6. Sampling and Analysis. Sediment resuspension was characterized by monitoring temporal changes in multiple physicochemical parameters. A brief overview is provided here, while comprehensive details are available in Note S2, Supporting Information.

Dissolved oxygen was measured directly in the sediment slurry using a probe (HQ30d, Hach). For additional analyses, approximately 55 mL of sediment slurry was centrifuged, and the supernatant was filtered for pH measurement using a pH meter (FE28 standard, electrode model LE438, Mettler Toledo), as well as for dissolved metal analysis (acidified) and alkalinity measurement (unacidified).[36] The sediment at the bottom of the centrifuge tube was analyzed for AVS and SEM concentrations using the purge-and-trap method.[37]

In situ porewater sampling was conducted by using microporous samplers. The initial 0.5 mL was discarded, and the subsequent 2 mL was acidified and stored for metal analysis. Porewater extracted during reequilibration (in *Experiment Run1* and *Run3*) was also examined for dissolved sulfide presence using a colorimetric reagent,[37] but no detectable color change was observed.

Clam tissue samples from the bioassay were freeze-dried and subjected to hot acid digestion in 0.5−1.0 mL of 65% HNO_3 at 80 °C for 8 h. The acid digest was diluted and analyzed by ICP−MS for the metal isotope concentration.

Metal concentrations of Mn, Fe, Ni, Cu, Zn, Cd, and Pb in water, porewater, DGT gel digest solutions, and sediment digest solutions were determined by ICP−MS. For organism tissue digest solutions, metal isotope concentrations (^{60}Ni, ^{62}Ni, ^{63}Cu, ^{65}Cu, ^{64}Zn, ^{68}Zn, ^{111}Cd, ^{114}Cd, ^{206}Pb, and ^{207}Pb) were analyzed. QA/QC procedures included monitoring internal reference standards for instrumental signal drift, measuring quality control standards every 15−20 samples,

https://doi.org/10.1021/acs.est.4c08327
Environ. Sci. Technol. XXXX, XXX, XXX−XXX

and analyzing certified reference materials (SRM 1566, oyster tissue) for overall quality control, ensuring recovery within 10% of reported values (detailed in Note S2, Supporting Information).

2.7. Isotopic Data Analysis. Metal bioavailability, as indicated by the assimilation rate, was quantified by tracking changes in metal isotopic concentration in clam tissue before and after sediment exposure. Core equations are presented here, with detailed derivations provided in Note S3 of the Supporting Information.

2.7.1. Newly Accumulated Concentration of Labeled Metal Isotopes in the Clams. During the isotopic-modification stage, clams were cultured in water spiked with labeled metal isotopes (i.e., ^{62}Ni, ^{65}Cu, ^{68}Zn, ^{114}Cd, and ^{206}Pb). The increase in labeled isotope concentration in the clam tissue ($^{L}\mathrm{Mel}_{new}$, μg g^{-1} dry weight) was calculated as (Note S3.1 for detailed explanation)[27]

$$ {}^{L}\mathrm{Mel}_{new} = ({}^{L}\mathrm{Mel}_{meas} - {}^{NL}\mathrm{Mel}_{meas}) \times f^{L} \quad (1) $$

where $^{L}\mathrm{Mel}_{meas}$ and $^{NL}\mathrm{Mel}_{meas}$ (μg g^{-1}) are the instrument-reported concentrations of labeled and nonlabeled isotopes, respectively, and f^{L} is the natural isotope abundance of labeled metal isotope (i.e., 3.63% for ^{62}Ni, 30.8% for ^{65}Cu, 18.8% for ^{68}Zn, 28.7% for ^{114}Cd, and 24.1% for ^{206}Pb).

2.7.2. Normalized Isotopic Ratio in the Clam. The accumulation of labeled isotopes in clam tissue resulted in the enrichment of these isotopes, indicated by elevated isotope ratios. The ratio $\mathrm{Me}^{L/NL}$ (i.e., $\mathrm{Ni}^{62/60}$, $\mathrm{Cu}^{65/63}$, $\mathrm{Zn}^{68/64}$, $\mathrm{Cd}^{114/111}$, and $\mathrm{Pb}^{206/207}$) was calculated as[26,27]

$$ \mathrm{Me}^{L/NL} = \frac{{}^{L}\mathrm{Mel}_{meas} \times f^{L}}{{}^{NL}\mathrm{Mel}_{meas} \times f^{NL}} \quad (2) $$

where f^{NL} is the natural isotope abundance of the nonlabeled isotope.

When exposed to metals in sediments, the clams absorb metal isotopes at their natural abundances, resulting in the dilution of the labeled isotope and a decrease in the $\mathrm{Me}^{L/NL}$ ratio. The mass of absorbed metal can be quantified by the decrease in the $\mathrm{Me}^{L/NL}$ ratio of the sediment exposure group relative to the reference group that was not exposed to contaminated sediments.[27] However, we observed that the decrease in $\mathrm{Me}^{L/NL}$ of some organism samples was influenced by variations in the enriching efficiency of the labeled isotope during the isotopic-modification stage (e.g., lower decrease of the $\mathrm{Me}^{L/NL}$ caused by higher enriching efficiency of labeled isotope).

To address variations in enrichment efficiency, we normalized the $\mathrm{Me}^{L/NL}$ ratio (R^{Me}_{norm}) by dividing $\mathrm{Me}^{L/NL}$ with the newly accumulated concentration of the labeled isotope ($^{L}\mathrm{Mel}_{new}$) of the same organism

$$ R^{Me}_{norm} = \frac{\mathrm{Me}^{L/NL} - f^{L/NL}}{{}^{L}\mathrm{Mel}_{new}} = \frac{\mathrm{Me}^{L/NL} - f^{L/NL}}{({}^{L}\mathrm{Mel}_{meas} - {}^{NL}\mathrm{Mel}_{meas}) \times f^{L}} \quad (3) $$

where $f^{L/NL}$ is the natural isotope abundance ratio between the labeled and nonlabeled metal isotope. R^{Me}_{norm} has a unit of g μg^{-1}. Although it can be converted to a dimensionless variable by multiplying it by 10^{6}, we retain this form for simplicity in calculating metal assimilation rates, as demonstrated below.

2.7.3. Metal Assimilation Rate Determined Following Sediment Exposure. In the sediment exposure group, the normalized R^{Me}_{norm} ratio ($R^{Me}_{norm}|_{exp}$) is the reciprocal of the sum of the background nonlabeled metal isotope fraction ($^{NL}\mathrm{Mel}_{bkg}$, μg g^{-1}) and the sedimentary source nonlabeled metal isotope fraction ($^{NL}\mathrm{Mel}_{sed}$, μg g^{-1}) (Note S3.3 for derivation)

$$ R^{Me}_{norm}|_{exp} = \frac{1}{{}^{NL}\mathrm{Mel}_{bkg} + {}^{NL}\mathrm{Mel}_{sed}} \quad (4) $$

In the reference group, where clams do not absorb metals from the sediment, the ratio ($R^{Me}_{norm}|_{base}$) is inversely related to that of $^{NL}\mathrm{Mel}_{bkg}$

$$ R^{Me}_{norm}|_{base} = \frac{1}{{}^{NL}\mathrm{Mel}_{bkg}} \quad (5) $$

Hence, the sedimentary source fraction ($^{NL}\mathrm{Mel}_{sed}$) can be calculated as

$$ {}^{NL}\mathrm{Mel}_{sed} = \frac{1}{R^{Me}_{norm}|_{exp}} - \frac{1}{R^{Me}_{norm}|_{base}} \quad (6) $$

Consequently, the total metal assimilation rate (AR_{Me}) during sediment exposure is then determined by

$$ \mathrm{AR}_{Me} = \frac{{}^{NL}\mathrm{Mel}_{sed}}{f^{NL} \times t_{exp}} \quad (7) $$

where t_{exp} (h) represents the duration of sediment exposure. AR_{Me} has a unit of μg g^{-1} h^{-1} and was converted to ng g^{-1} h^{-1}.

3. RESULTS AND DISCUSSION

3.1. *Experiment Run1*: Sediment Resuspension Oxidized Reducing Sediments and Enhanced Metal Release. Sediment resuspension rapidly oxidized the sediment slurry in *Experiment Run1*, evidenced by a substantial decrease in dissolved Fe and AVS within 2 h. Dissolved Fe decreased from 800 to 300 μg L^{-1}, while AVS decreased from 38 to 4.4 μmol g^{-1} (Figures S1 and S2, Supporting Information). This decline continued over the next 10 to 22 h, reaching 90 μg L^{-1} for Fe and 0.5 μmol g^{-1} for AVS, and remained low thereafter. The rapid oxidation of these reducing substances corresponded to an initially very low DO concentration (<0.2 mg L^{-1}) in the sediment slurry (Figure S3, Supporting Information), indicating rapid oxygen consumption by the oxidation process. DO gradually recovered to 3.6 mg L^{-1} from 24 h until the experiment's completion on day 7, suggesting a gradual shift to oxidized condition during the later stage of sediment resuspension.

During resuspension, the continuous oxidation of mineral sulfides releases protons, contributing to acidity.[38] However, substantial acidification of the sediment slurry did not occur; the pH slightly decreased from 7.8 to 6.5 (Figure S3). This was attributed to the buffering capacity of both sediment and water, as evidenced by a gradual decrease in dissolved alkalinity from 4.5 to 0.9 mmol L^{-1} throughout the resuspension duration.

Sediment oxidation released Ni, Cu, Zn, and Cd into the aqueous phase but not Pb. Initial concentrations of dissolved Ni, Cu, Zn, and Cd were low but gradually increased to 380, 20, 220, and 1.6 μg L^{-1}, respectively, by the end of resuspension (Figure S1). Release of Pb was not observed, likely due to the low solubility of Pb-bearing phases.

While SEM concentrations can provide insight into the change of particulate metal speciation during sediment

https://doi.org/10.1021/acs.est.4c08327
Environ. Sci. Technol. XXXX, XXX, XXX−XXX

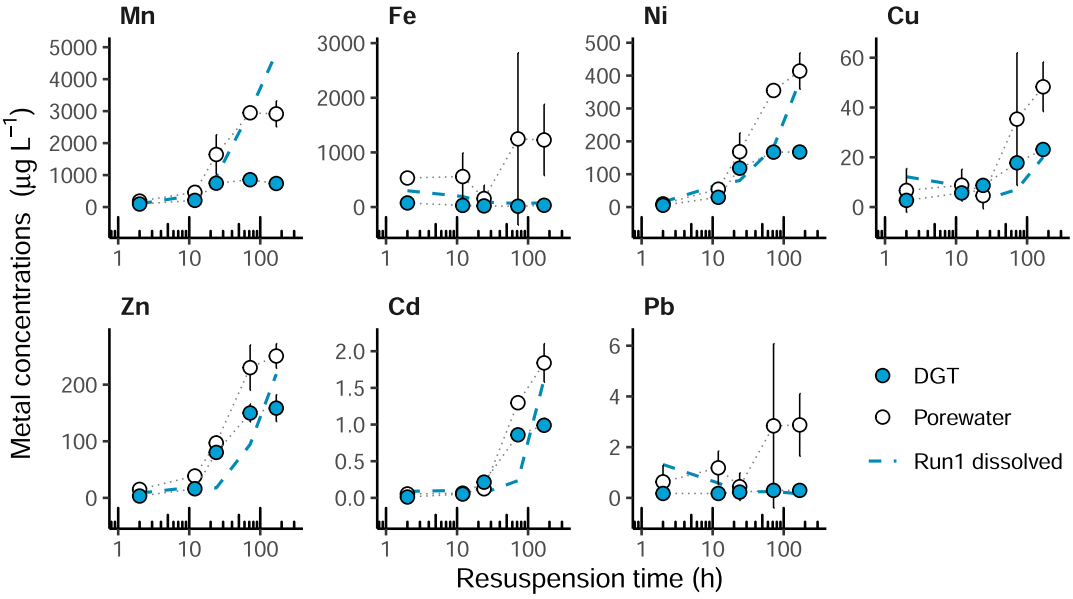

Figure 1. Sediment resuspension releases metals into porewater, as indicated by increasing concentrations of porewater metals and DGT-labile metals over time in *Experiment Run2*. Results are presented as mean (points connected by dotted lines) and standard deviation (error bars) of triplicate test results for each time interval. The blue dashed lines represent the mean dissolved metal concentrations in *Experiment Run1* (refer to Figure S1 for details, Supporting Information).

oxidation (Figure S2), the interpretability of these results is affected by subsampling artifacts. During subsampling, finer materials enriched with Fe and Mn were preferentially collected, leading to misleading trends in the observed SEM concentrations. Unexpectedly, SEM-Fe and SEM-Mn decreased with resuspension time, contradicting expectations of stable SEM concentrations given the high solubility of particulate Fe and Mn phases in diluted HCl (1 M). We attribute these decreasing trends to the subsampling effect, where the selective capture of finer particles resulted in the loss of coarser materials that settled at the flask bottom.

Given the subsampling effect, the SEM results during sediment resuspension are presented but are not fully interpreted. However, notable differences emerged in the temporal trends of SEM-Cu and SEM-Ni compared to SEM-Fe and SEM-Mn (Figure S2), qualitatively shedding light on the speciation change of Cu and Ni during resuspension. Specifically, SEM-Cu increased for the first 24 h and remained constant thereafter, while SEM-Ni remained approximately constant throughout the resuspension experiment. Cu and Ni solid phases typically exist as sulfide phases when there is a molar excess of AVS, as exhibited in these contaminated sediments.[39] Both Cu and Ni sulfide exhibit low solubility in 1 M HCl, resulting in incomplete extraction during SEM and AVS analysis.[15,40] Yet, when oxidized, they become more soluble. Therefore, the diverging trends of SEM-Cu and SEM-Ni from SEM-Fe and SEM-Mn (easily extractable phases) indicate an increasing abundance of 1 M HCl-extractable Cu and Ni within the sediments, suggesting ongoing oxidation of Cu and Ni-bearing species during sediment resuspension.

3.2. *Experiment Run2*: Metal Partitioning between Porewater and Redeposited Sediment Instantly (2 h) Following Resuspension. Porewater metal concentrations (determined by in situ extraction) and DGT-labile metal concentrations revealed shifts in the partitioning dynamics of metals in redeposited sediments shortly after resuspension.

Short-term resuspension pretreatment induced a limited release of metals into porewater (Figure 1). Cu, Cd, and Pb concentrations remained low within the first 24 h, while Mn, Ni, and Zn remained low for the first 12 h. Extended resuspension mobilized more metals, with porewater concentrations increasing to 2900, 410, 48, 250, 1.8, and 2.9 $\mu g\ L^{-1}$ for Mn, Ni, Cu, Zn, Cd, and Pb, respectively, after 168 h of resuspension.

Comparable concentration ranges and trends were observed between porewater metals in *Experiment Run2* (2 h of sediment settling +10 h of bioassay deployment) and dissolved metals in *Experiment Run1* (after different resuspension intervals) (Figure 1). The consistency suggests that a short reequilibration process did not substantially alter metal partitioning, and temporal changes in porewater metal concentrations were primarily influenced by resuspension duration.

DGT-labile concentrations showed trends similar to those of porewater metal concentrations (Figure 1). As the resuspension time increased from 2 to 168 h, DGT-labile metal concentrations increased from 95 to 740 $\mu g\ L^{-1}$ for Mn, from 5.4 to 170 $\mu g\ L^{-1}$ for Ni, from 2.7 to 23 $\mu g\ L^{-1}$ for Cu, from 3.2 to 150 $\mu g\ L^{-1}$ for Zn, and from 0.01 to 1.0 $\mu g\ L^{-1}$ for Cd. DGT-labile concentrations of Fe and Pb remained constantly low (approximately 30 $\mu g\ L^{-1}$ for Fe and 0.2 $\mu g\ L^{-1}$ for Pb) regardless of the resuspension time.

DGT-labile metal concentrations encompass metals in the porewater and those resupplied from weakly bound sediment pools. With a fast resupply (the sustained case), DGT-labile metal concentrations are comparable to the porewater metal concentrations.[34] Otherwise, in less sustained conditions, DGT-labile concentrations are lower. Here, although similar trends were observed between DGT-labile concentrations and porewater Mn, Ni, Cu, Zn, and Cd, DGT-labile concentrations were lower at longer resuspension durations (Figure 1). This suggests that extended resuspension released more mobile metals into the porewater, while particulate metals did not

https://doi.org/10.1021/acs.est.4c08327
Environ. Sci. Technol. XXXX, XXX, XXX−XXX

sustain well porewater concentrations when depleted by the DGT samplers.

3.3. *Experiment Run2*: Impact of Sediment Resuspension on Metal Bioavailability in Redeposited Sediments. Increased concentrations of labeled isotopes and elevated isotope ratios during the isotopic modification stage indicate effective enrichment in labeled isotopes (Figures S4 and S5, Supporting Information).

Following sediment exposure, the normalized isotopic ratios of $Ni^{62/60}$ and $Pb^{206/207}$ were significantly lower than the baseline ratios of the reference group, indicating significant detection of bioavailable Ni and Pb in the sediment ($p < 0.05$, one-way ANOVA, Figure S6, Supporting Information). These ratios decreased with longer resuspension times. Similarly, the normalized isotopic ratio of $Cu^{65/63}$ was also lower than the baseline, though less significantly ($p > 0.05$, one-way ANOVA, Figure S6), suggesting bioavailable Cu was present but nearing the detection limit of the bioassay.

In contrast, the normalized isotopic ratios of $Cd^{114/111}$ and $Zn^{68/64}$ did not show systematic differences from the reference group ($p > 0.05$, one-way ANOVA, Figure S6). The $Cd^{114/111}$ ratio varied within one standard deviation of the mean baseline ratio, implying low Cd bioavailability. For Zn, the $Zn^{68/64}$ ratios were 1 to 3 orders of magnitude lower than those observed for other metals due to high background Zn concentrations in clam tissue, leading to inefficient isotope enrichment (Figure S5).[26] Consequently, this approach showed low sensitivity for the detection of Zn bioavailability.

The variations in isotopic ratios reflect dynamic changes in metal bioavailability, as shown by the metal assimilation rates in clams after different sediment resuspension durations (Figure 2a). For short-duration resuspension, the assimilation rates of Ni, Cu, and Pb remained low, approximately 7.3 ng g^{-1} h^{-1} for Ni within the first 12 h, 140 ng g^{-1} h^{-1} for Cu within the first 24 h, and 3.0 ng g^{-1} h^{-1} for Pb within the first 12 h. This indicates minimal enhancement in metal bioavailability during short-term resuspension.

Extended resuspension increased the metal bioavailability. After 168 h resuspension, mean assimilation rates for Ni and Pb were 3 and 2.6 times higher than those after 2 h resuspension. Similarly, mean Cu assimilation rates increased 2.7 times following 72 h of resuspension but slightly decreased to 1.6 times following 168 h of resuspension.

3.4. *Experiment Run1* and *Run3*: Gradual Recovery of Porewater Metal Chemistry during Sediment Reequilibration. Porewater metal concentrations revealed consistent temporal changes during the reequilibration phase following a 7 d resuspension. This was observed with both continuous equilibration from the same batch of resuspended sediments (*Experiment Run1*, Figure S7, Supporting Information) and prescheduled equilibration from different resuspension batches (*Experiment Run3*, Figure 3).

Throughout the reequilibration phase, porewater Fe concentrations remained consistently low for 14 days in *Experiment Run1* and 7 days in *Experiment Run3* (Figures S7 and 3). These levels were much lower than preresuspension, indicating the predominant solid-phase Fe(III) in the sediment with minimal reduction to dissolved Fe(II). The absence of dissolved sulfide in the porewater (Section 2.6) further corroborated the absence of the reducing conditions.

During reequilibration, porewater concentrations of Ni, Cu, Zn, and Cd decreased over time (Figures 3 and S7), likely due to adsorption by the Fe(III) oxide solid phase. In *Experiment Run3* (Figure 3), Cu, Zn, and Cd concentrations decreased to preresuspension levels after 72 h of equilibration and remained stable. However, porewater Ni approached a constant concentration (71 μg L^{-1}), significantly higher than its preresuspension level (7 μg L^{-1}). Porewater Pb remained stable and below its preresuspension level throughout the reequilibration phase.

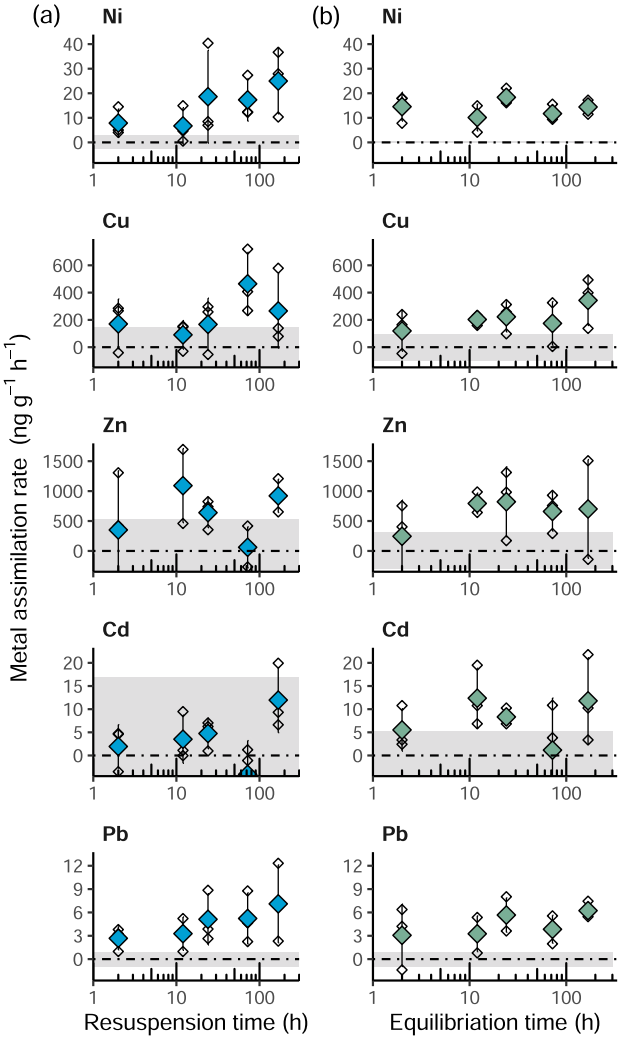

Figure 2. Dynamics in metal bioavailability, indicated by metal assimilation rates, in nonequilibrium sediments. (a) Change in metal assimilation rates over different resuspension durations. (b) Metal assimilation rates either remain unchanged or slightly increase over reequilibration time. Each hollow diamond point represents the mean assimilation rate for seven clams in each replicate test. The solid diamond points and error bars represent the mean and the standard deviation of the three replicates. The shaded areas indicate the detection limit for bioavailability, derived from the mean ratio and the standard deviation of the reference group.

DGT-labile metal concentrations from piston DGTs in *Experiment Run1* mirrored the trends of porewater metal concentrations, with decreases observed for Ni, Cu, Zn, and Cd, and consistently low levels for Fe and Pb (Figure S7).

Planar DGT probes in *Experiment Run3* provided depth profiles of labile metal concentrations across the sediment–water interface (SWI) (Figure S8, Supporting Information). DGT-labile Fe(II) remained consistently low across all depths, confirming the absence of Fe(III) reduction. Mn, Ni, Cu, Zn, and Cd displayed typical depth profiles,[39,41] with higher

https://doi.org/10.1021/acs.est.4c08327
Environ. Sci. Technol. XXXX, XXX, XXX−XXX

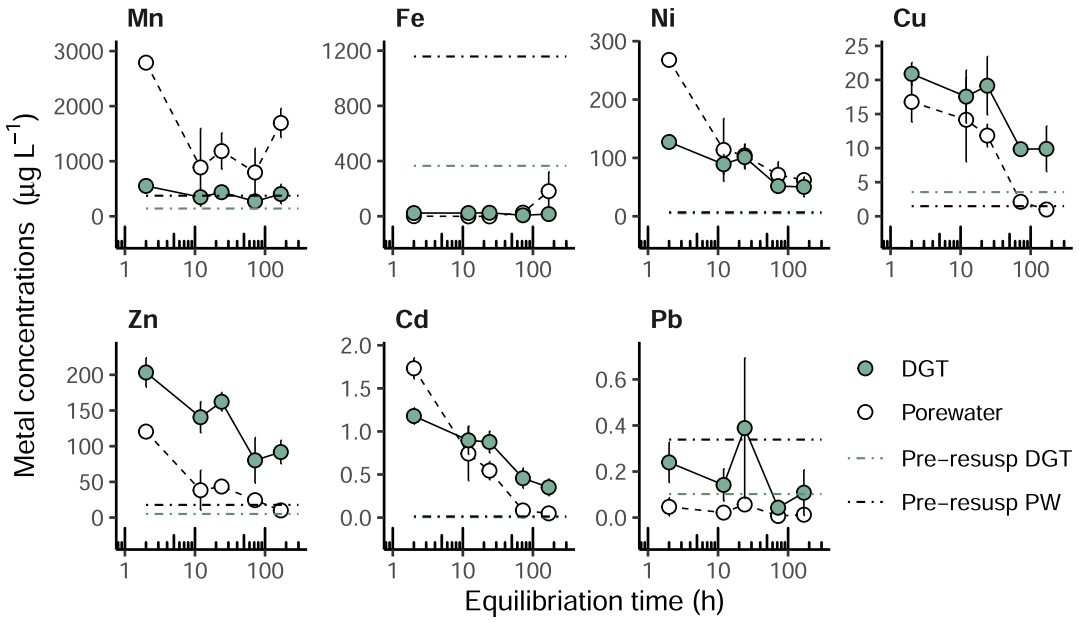

Figure 3. Sediment reequilibration scavenges metals from porewater, as indicated by decreasing concentrations of DGT-labile metals and porewater metals over time in *Experiment Run3*. Results are presented as mean values with standard deviations from triplicate test results for each time interval. The horizontal dashed lines represent the preresuspension levels of porewater metal and DGT-labile metals, determined separately in sediments not subjected to resuspension.

concentrations in surficial porewater than in overlying water, creating a concentration gradient across the SWI (Figure S8). Over time, their concentrations in the overlying water remained low, while their concentrations in porewater decreased.

Depth-averaged (depths below the SWI) concentrations of DGT-labile metals from planar DGT probes (in *Experiment Run3*, Figure S8) showed temporal patterns (ranges and trends) similar to those from piston DGT samplers in *Experiment Run1* (Figure S7). This similarity (Figure S9, Supporting Information) highlights reproducible geochemical conditions controlling metal partitioning during reequilibration, irrespective of the equilibration approaches employed.

During reequilibration, the depth-averaged concentrations of DGT-labile metals (in *Experiment Run3*) were comparable to (for Ni, Cd, and Pb) or slightly higher (for Cu and Zn) than porewater metal concentrations (Figure 3). This suggests a rapid resupply from sediments to porewater when porewater metals were depleted (well-sustained condition). These results contrast with the low and/or slow resupply observed immediately after the resuspension period (Figure 1), indicating that metals immobilized onto the particulate phase during sediment reequilibration may remain in a more mobile pool.

3.5. *Experiment Run3*: Unanticipated Trends in the Metal Bioavailability Dynamics during Sediment Reequilibration. During sediment reequilibration, the mean normalized isotopic ratios of $Ni^{62/60}$, $Cu^{65/63}$, $Zn^{68/64}$, $Cd^{114/111}$, and $Pb^{206/207}$ were consistently lower than their respective reference ratios (Figure S10, Supporting Information). The differences were more significant for the ratios of $Ni^{62/60}$, $Cu^{65/63}$, and $Pb^{206/207}$, while they were less significant for $Zn^{68/64}$ and $Cd^{114/111}$ (Figure S10). The persistent pattern indicates the bioavailability of these metals to the clams within the sedimentary system. Given that metal concentrations in the overlying water remained low during the bioassay exposure, as evidenced by the low DGT-labile concentrations above the SWI (Figure S8), it is clear that the source of these bioavailable metals is sediments, encompassing both porewater and sediment particles.

At the shortest sediment equilibration interval (2 h of sediment settling +10 h of bioassay deployment) (Figure 2b, initial points), assimilation rates were lower than those measured at the longest interval of sediment resuspension in *Experiment Run2* (Figure 2a, final points). Despite both sets of sediments undergoing identical durations of resuspension (7 d) and reequilibration (12 h), subtle differences between independent experimental conditions likely contribute to this discrepancy in assimilation rates. This difference is also reflected in the discrepancies observed in porewater metal concentrations (Figure 1 and Figure 3). Therefore, it is essential to focus on the trends of assimilation rates within each independent experiment to understand the dynamics of the metal bioavailability.

Throughout the reequilibration phase, assimilation rates either remained relatively constant or exhibited a slight increase (Figure 2b). Specifically, the assimilation rates varied between 10 and 18 ng g^{-1} $h^{-1}$for Ni, between 1.2 and 12 ng g^{-1} h^{-1} for Cd, and between 3.1 and 6.2 ng g^{-1} h^{-1} for Pb. The assimilation rates of Cu slightly increased with equilibration time, while the assimilation rates of Zn initially increased from 250 ± 600 to 790 ± 180 ng g^{-1} h^{-1} within 12 h and then remained stable thereafter. These trends in metal assimilation rates during reequilibration defy the anticipated declining trends of metal bioavailability predicted solely based on porewater metal concentrations.

3.6. Linking Metal Biogeochemical Processes with Bioavailability Dynamics. The conventional understanding of variations in metal bioavailability under dynamic environmental conditions often relies on simplistic deductions drawn from the chemical characterization of metal biogeochemistry. We observed that sediment resuspension mobilized metals to

https://doi.org/10.1021/acs.est.4c08327
Environ. Sci. Technol. XXXX, XXX, XXX−XXX

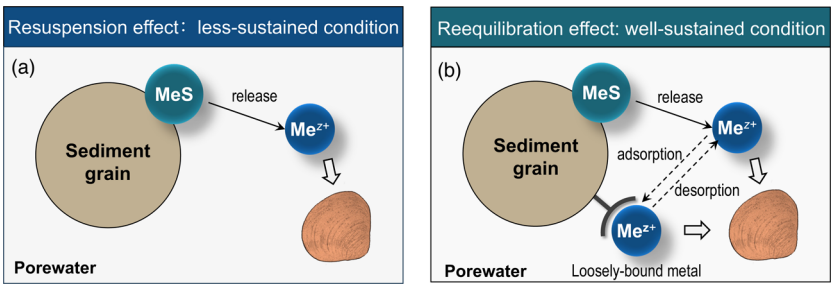

Figure 4. Schematic of processes that control metal bioavailability in sediment under different disturbed scenarios.

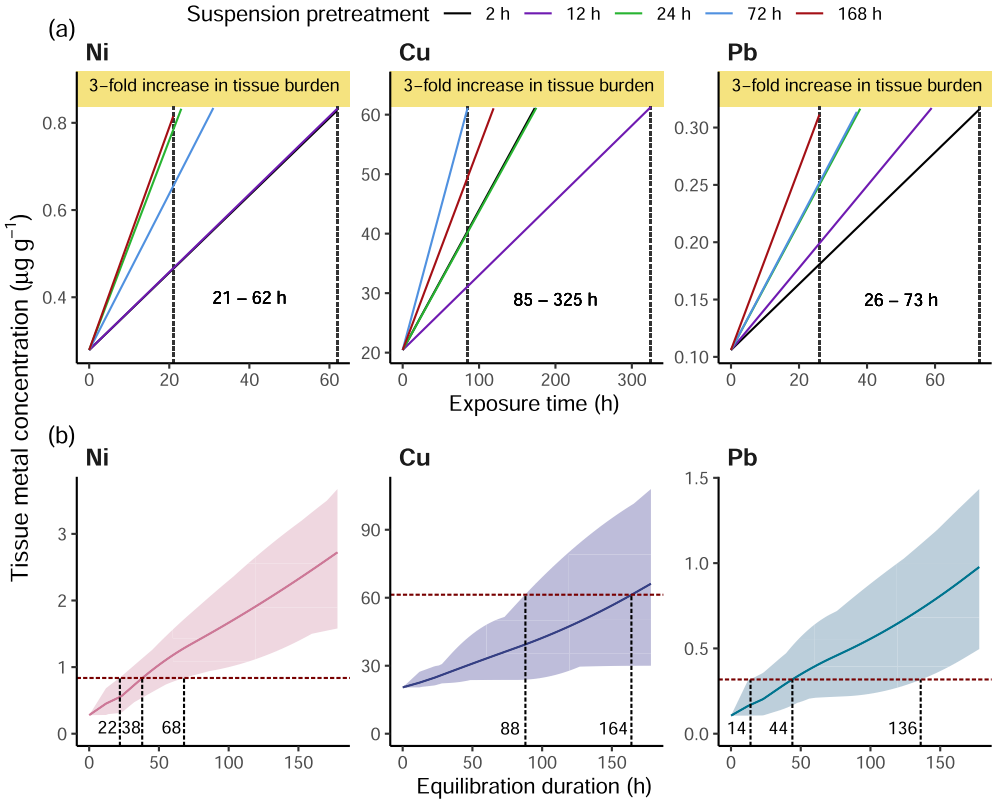

Figure 5. Toxicokinetic model predictions of metal bioaccumulation in clams under varying bioavailability conditions influenced by different resuspension (a) and reequilibration (b) durations. In (a), solid lines represent model-predicted bioaccumulation curves for different resuspension durations, with vertical dashed lines indicating the minimum and maximum times required for a 3-fold increase in tissue concentrations. In (b), the shaded areas indicate the higher-bound and the lower-bound of predicted bioaccumulation curves, solid lines represent mean bioaccumulation curves, horizontal dashed lines mark a 3-fold increase in baseline tissue concentrations, and vertical dashed lines correspond to the time required for a 3-fold increase.

the porewater through the ongoing oxidation of metal-contaminated sediments and subsequent reequilibration immobilized metals via scavenging metals from porewater.

Based on these porewater measurements, we expected increased metal bioavailability during sediment resuspension and decreased bioavailability during reequilibration. The isotopically modified bioassay measurements revealed bioavailability dynamics that aligned with porewater metal chemistry for Ni (r = 0.9, p < 0.05 for DGT-labile Ni and for porewater Ni) and Pb (r = 0.9, p < 0.05 for DGT-labile Pb) during the resuspension phase (Figures S11 and S12, Supporting Information). However, this hypothesis was partially rejected as the correlation for Cu was less significant (r = 0.69, p = 0.20, Figure S11). Additionally, during sediment reequilibration, the observed decrease in porewater metals, indicative of metal immobilization, did not correspond to reduced metal bioavailability, as shown by the lack of correlations (p > 0.05, Figures S13 and S14, Supporting Information). This indicates that while our hypothesis held during resuspension for certain metals, it did not apply during reequilibration.

The inconsistency may be qualitatively explained by considering the sustained release of metals from the particulate phase to porewater during the reequilibration phase (Figure 4). While ongoing immobilization occurred during sediment reequilibration, the immobilized fraction of metals might remain "active" to the organism, as inferred from the higher sustaining capability (Figure 3). Therefore, when clams are exposed to such sediments, the more recently immobilized metals in this "active" pool may still be bioavailable (Figure 4b),[42] either by supplying to porewater when dissolved metals at the organism interface are depleted or by direct absorption when sediments are ingested.

https://doi.org/10.1021/acs.est.4c08327
Environ. Sci. Technol. XXXX, XXX, XXX−XXX

In contrast, during the sediment resuspension phase, particularly under longer resuspension durations, metals in the porewater were less sustained (Figure 1) because metals on sediment particles were more tightly bound. In such conditions, the clams may primarily take up metals through aqueous exposure (Figure 4a), and the DGT-labile metals may define the upper limit of metals assimilable in the sedimentary system.

3.7. Environmental Relevance and Implications on Risk Assessment of Metal-Contaminated Sediments. Anthropogenic activities, such as dredging, significantly disrupt the sediment structure, releasing suspended sediments into the water column. Even after settling, repetitive suspension of surficial sediments,[43] driven by wind and wave action, may lead to extended oxidation of reducing sediments. This resuspension and subsequent reequilibration can notably alter the bioavailability of contaminants.

Our findings highlight discrepancies between traditional assessments based on porewater analysis and the assimilation rates measured using the isotopically modified bioassay. These discrepancies suggest that metal bioavailability may differ from previous understandings under nonequilibrium conditions, challenging existing paradigms regarding sediment-associated metal contamination risks.[7] By introducing the isotopically modified bioassay, we provide a significant advancement for quantitatively determining metal bioavailability within short-time windows. This approach effectively captures transient fluctuations in metal bioavailability, allowing for the integration of dynamic changes into kinetic models and enhancing the assessment of metal risks under nonequilibrium conditions.

The measured assimilation rates represent the combined metal accumulation from different pathways in the sedimentary environment, simplifying the construction of toxicokinetic models by eliminating the need to separately account for metal uptake from each pathway.[28] This streamlined approach is particularly useful for assessing risks associated with contaminated sediments, where distinction of uptake pathways may not be critical.[28] Incorporating assimilation rates into toxicokinetic models thus enables bioaccumulation risk assessment under simulated resuspension and reequilibration events (Notes S4.1, Supporting Information).

Assessing bioaccumulation risk has formed a part of sediment quality assessment practices, typically based on comparing tissue concentration with threshold concentrations.[25,44] However, current threshold derivation (e.g., 3-fold increase relative to control exposure[44]) remains arbitrary or mechanistically unfounded. This can be improved by considering baseline concentrations and adverse effect information (e.g., maximum residue limit).[45] For simplicity, we used a 3-fold increase in baseline tissue concentration to indicate risk,[45] while other mechanistically derived thresholds can also be used to assess bioaccumulation risks.

To assess the effect of resuspension on metal bioaccumulation risks in sediments, we simulated the bioaccumulation to the clam with bioavailability levels influenced by different resuspension and reequilibration durations (Note S4.2). We predicted the time required for a 3-fold increase (TRI-time) in tissue concentrations under each condition (Note S4.3). The toxicokinetic model predicted that resuspension substantially decreases TRI-time for Ni, Cu, and Pb, by approximately 3-fold (Figure 5a). Notably, the TRI-time for Ni and Pb are as short as 21 and 26 h, respectively, underscoring the potential for rapid and concerning accumulation.

During the 7 d reequilibration following 7 d resuspension, the predicted tissue metal concentrations increased steadily over the 168 h reequilibration phase (Figure 5b and Figure S15, Supporting Information). For the contaminated sediment modeled, tissue metal concentrations readily exceed the 3-fold increase threshold for Ni (within 22−68 h), Cu (88−164 h or longer), and Pb (14−136 h) (Figure 5b) and approach this threshold for Zn and Cd (Figure S15). Notably, the mean tissue concentrations of Ni and Pb reached this threshold within just 48 h. This indicates that even after sediments have settled and reequilibrated following a heavy suspension, the risk of metal bioaccumulation persists for an extended duration, posing ongoing threats to benthic organisms. This finding aligns with our previous study, where disturbed sediments subjected to a week of oxidation exhibited elevated toxicity to benthic amphipod species, even after an additional 4 weeks of equilibration.[46]

Overall, our study highlights the complexity of the metal bioavailability in sediments disturbed by resuspension. In such nonequilibrium scenarios, establishing a quantitative relationship between metal bioavailability and simple chemical measurements is challenging. Relying solely on chemical analysis of porewater may overlook the "ghosting" pool of bioavailable metals on sediment grains, potentially biasing and underestimating risk prediction outcomes. The isotopically modified bioassay provides direct information on metal bioavailability through measured assimilation rates. These rates can be integrated into toxicokinetic models to predict metal bioaccumulation under various nonequilibrium conditions. Therefore, incorporating dynamic bioavailability measurements in risk assessment models could potentially improve prediction accuracy in nonequilibrium sediments and inform sediment management strategies more effectively.

■ ASSOCIATED CONTENT

Supporting Information

The Supporting Information is available free of charge at https://pubs.acs.org/doi/10.1021/acs.est.4c08327.

Detailed description of the methods for DGT application and analysis, sediment sampling and metal analysis, stable isotope analysis of metals, characterization of sediment resuspension, effects of reequilibration on porewater metal chemistry, impact of resuspension and reequilibration on metal bioavailability, and construction of a toxicokinetic model for predicting metal bioaccumulation (PDF)

■ AUTHOR INFORMATION

Corresponding Author

Minwei Xie − *Fujian Provincial Key Laboratory for Coastal Ecology and Environmental Studies, State Key Laboratory of Marine Environmental Science, Key Laboratory of the Ministry of Education for Coastal and Wetland Ecosystem, College of the Environment and Ecology, Xiamen University, Xiamen, Fujian 361102, China;* orcid.org/0000-0003-4359-8738; Email: minweixie@xmu.edu.cn

Authors

Dejin Xu − *Fujian Provincial Key Laboratory for Coastal Ecology and Environmental Studies, State Key Laboratory of Marine Environmental Science, Key Laboratory of the Ministry of Education for Coastal and Wetland Ecosystem,*

https://doi.org/10.1021/acs.est.4c08327
Environ. Sci. Technol. XXXX, XXX, XXX−XXX

College of the Environment and Ecology, Xiamen University, Xiamen, Fujian 361102, China

Haiyan Xiong − *Fujian Provincial Key Laboratory for Coastal Ecology and Environmental Studies, State Key Laboratory of Marine Environmental Science, Key Laboratory of the Ministry of Education for Coastal and Wetland Ecosystem, College of the Environment and Ecology, Xiamen University, Xiamen, Fujian 361102, China*

Qiuling Wu − *Fujian Provincial Key Laboratory for Coastal Ecology and Environmental Studies, State Key Laboratory of Marine Environmental Science, Key Laboratory of the Ministry of Education for Coastal and Wetland Ecosystem, College of the Environment and Ecology, Xiamen University, Xiamen, Fujian 361102, China*

Wenze Xiao − *Fujian Provincial Key Laboratory for Coastal Ecology and Environmental Studies, State Key Laboratory of Marine Environmental Science, Key Laboratory of the Ministry of Education for Coastal and Wetland Ecosystem, College of the Environment and Ecology, Xiamen University, Xiamen, Fujian 361102, China*

Stuart L. Simpson − *CSIRO Environment, Ecosciences Precinct, Dutton Park, Queensland 4102, Australia*

Qiao-Guo Tan − *Fujian Provincial Key Laboratory for Coastal Ecology and Environmental Studies, State Key Laboratory of Marine Environmental Science, Key Laboratory of the Ministry of Education for Coastal and Wetland Ecosystem, College of the Environment and Ecology, Xiamen University, Xiamen, Fujian 361102, China;* orcid.org/0000-0001-9692-6622

Rong Chen − *Fujian Provincial Key Laboratory for Coastal Ecology and Environmental Studies, State Key Laboratory of Marine Environmental Science, Key Laboratory of the Ministry of Education for Coastal and Wetland Ecosystem, College of the Environment and Ecology, Xiamen University, Xiamen, Fujian 361102, China*

Complete contact information is available at: https://pubs.acs.org/10.1021/acs.est.4c08327

Author Contributions

[§]D.X. and H.X. contributed equally.

Notes

The authors declare no competing financial interest.

■ ACKNOWLEDGMENTS

This study was supported by the National Natural Science Foundation of China (Grant Nos. 42077372 and 42477281).

■ REFERENCES

(1) Kalnejais, L. H.; Martin, W. R.; Signell, R. P.; Bothner, M. H. Role of sediment resuspension in the remobilization of particulate-phase metals from coastal sediments. *Environ. Sci. Technol.* **2007**, *41* (7), 2282−2288.

(2) Eggleton, J.; Thomas, K. V. A review of factors affecting the release and bioavailability of contaminants during sediment disturbance events. *Environ. Int.* **2004**, *30* (7), 973−980.

(3) Cao, X.; Yu, Z.-X.; Xie, M.; Pan, K.; Tan, Q.-G. Higher Risks of Copper Toxicity in Turbid Waters: Quantifying the Bioavailability of Particle-Bound Metals to Set Site-Specific Water Quality Criteria. *Environ. Sci. Technol.* **2023**, *57* (2), 1060−1070.

(4) Fetters, K. J.; Costello, D. M.; Hammerschmidt, C. R.; Burton, G. A. Toxicological effects of short-term resuspension of metal-contaminated freshwater and marine sediments. *Environ. Toxicol. Chem.* **2016**, *35*, 676−686.

(5) Cervi, E. C.; Hudson, M.; Rentschler, A.; Burton, G. A. Metal Toxicity During Short-Term Sediment Resuspension and Redeposition in a Tropical Reservoir. *Environ. Toxicol. Chem.* **2019**, *38* (7), 1476−1485.

(6) Hill, N. A.; King, C. K.; Perrett, L. A.; Johnston, E. L. Contaminated suspended sediments toxic to an Antarctic filter feeder: Aqueous- and particulate-phase effects. *Environ. Toxicol. Chem.* **2009**, *28* (2), 409−417.

(7) Burton Jr, G. A. Sediment quality criteria in use around the world. *Limnology* **2002**, *3* (2), 65−76.

(8) Burton, G. A.; Pitt, R.; Clark, S. The Role of Traditional and Novel Toxicity Test Methods in Assessing Stormwater and Sediment Contamination. *Crit. Rev. Environ. Sci. Technol.* **2000**, *30* (4), 413−447.

(9) Di Toro, D. M.; Mahony, J. D.; Hansen, D. J.; Scott, K. J.; Carlson, A. R.; Ankley, G. T. Acid volatile sulfide predicts the acute toxicity of cadmium and nickel in sediments. *Environ. Sci. Technol.* **1992**, *26* (1), 96−101.

(10) Simpson, S. L.; Batley, G. E. Predicting metal toxicity in sediments: a critique of current approaches. *Integrated Environ. Assess. Manag.* **2007**, *3* (1), 18−31.

(11) USEPA. *Procedures for the Derivation of Equilibrium Partitioning Sediment Benchmarks (ESBs) for the Protection of Benthic Organisms: Metal Mixtures (Cadmium, Copper, Lead, Nickel, Silver, and Zinc)*; US Environmental Protection Agency, Office of Research and Development: Washington, DC, USA, 2005.

(12) Peiffer, S.; Kappler, A.; Haderlein, S. B.; Schmidt, C.; Byrne, J. M.; Kleindienst, S.; Vogt, C.; Richnow, H. H.; Obst, M.; Angenent, L. T.; Bryce, C.; McCammon, C.; Planer-Friedrich, B. A biogeochemical−hydrological framework for the role of redox-active compounds in aquatic systems. *Nat. Geosci.* **2021**, *14*, 264−272.

(13) Rickard, D.; Morse, J. W. Acid volatile sulfide (AVS). *Mar. Chem.* **2005**, *97* (3), 141−197.

(14) Hong, Y. S.; Kinney, K. A.; Reible, D. D. Acid volatile sulfides oxidation and metals (Mn, Zn) release upon sediment resuspension: Laboratory experiment and model development. *Environ. Toxicol. Chem.* **2011**, *30* (3), 564−575.

(15) Simpson, S. L.; Apte, S. C.; Batley, G. E. Effect of short-term resuspension events on trace metal speciation in polluted anoxic sediments. *Environ. Sci. Technol.* **1998**, *32* (5), 620−625.

(16) Simpson, S. L.; Apte, S. C.; Batley, G. E. Effect of short-term resuspension events on the oxidation of cadmium, lead, and zinc sulfide phases in anoxic estuarine sediments. *Environ. Sci. Technol.* **2000**, *34* (21), 4533−4537.

(17) Xie, M.; Alsina, M. A.; Yuen, J.; Packman, A. I.; Gaillard, J.-F. Effects of resuspension on the mobility and chemical speciation of zinc in contaminated sediments. *J. Hazard. Mater.* **2019**, *364*, 300−308.

(18) Van Cappellen, P.; Gaillard, J.-F.; Rabouille, C. Biogeochemical Transformations in Sediments: Kinetic Models of Early Diagenesis. In *Interactions of C, N, P and S Biogeochemical Cycles and Global Change*; Wollast, R., Mackenzie, F. T., Chou, L., Eds.; Springer Berlin Heidelberg: Berlin, Heidelberg, 1993; pp 401−445.

(19) Gaillard, J.-F.; Jeandel, C.; Michard, G.; Nicolas, E.; Renard, D. Interstitial water chemistry of Villefranche Bay sediments: trace metal diagenesis. *Mar. Chem.* **1986**, *18* (2), 233−247.

(20) Xie, M.; Jarrett, B. A.; Da Silva-Cadoux, C.; Fetters, K. J.; Burton, G. A.; Gaillard, J.-F.; Packman, A. I. Coupled effects of hydrodynamics and biogeochemistry on Zn mobility and speciation in highly contaminated sediments. *Environ. Sci. Technol.* **2015**, *49* (9), 5346−5353.

(21) Burton, G. A. Metal bioavailability and toxicity in sediments. *Crit. Rev. Environ. Sci. Technol.* **2010**, *40* (9−10), 852−907.

(22) Chapman, P. M.; Wang, F. Assessing sediment contamination in estuaries. *Environ. Toxicol. Chem.* **2001**, *20* (1), 3−22.

(23) Simpson, S. L.; Spadaro, D. A.; O'Brien, D. Incorporating bioavailability into management limits for copper in sediments contaminated by antifouling paint used in aquaculture. *Chemosphere* **2013**, *93* (10), 2499−2506.

(24) Leppanen, M. T.; Sourisseau, S.; Burgess, R. M.; Simpson, S. L.; Sibley, P.; Jonker, M. T. Sediment toxicity tests: A critical review of their use in environmental regulations. *Environ. Toxicol. Chem.* **2024**, *43* (8), 1697−1716.
(25) Amato, E. D.; Marasinghe Wadige, C. P. M.; Taylor, A. M.; Maher, W. A.; Simpson, S. L.; Jolley, D. F. Field and laboratory evaluation of DGT for predicting metal bioaccumulation and toxicity in the freshwater bivalve Hyridella australis exposed to contaminated sediments. *Environ. Pollut.* **2018**, *243*, 862−871.
(26) Wu, Q.; Zheng, T.; Simpson, S. L.; Tan, Q.-G.; Chen, R.; Xie, M. Application of a multi-metal stable-isotope-enriched bioassay to assess changes to metal bioavailability in suspended sediments. *Environ. Sci. Technol.* **2021**, *55* (19), 13005−13013.
(27) Wu, Q.; Su, Q.; Simpson, S. L.; Tan, Q.-G.; Chen, R.; Xie, M. Isotopically modified bioassay bridges the bioavailability and toxicity risk assessment of metals in bedded sediments. *Environ. Sci. Technol.* **2022**, *56* (23), 16919−16928.
(28) Su, Q.; Xiao, W.; Simpson, S. L.; Tan, Q.-G.; Chen, R.; Xie, M. Enhancing Sediment Bioaccumulation Predictions: Isotopically Modified Bioassay and Biodynamic Modeling for Nickel Assessment. *Environ. Sci. Technol.* **2023**, *57* (48), 19352−19362.
(29) Croteau, M. N.; Cain, D. J.; Fuller, C. C. Novel and nontraditional use of stable isotope tracers to study metal bioavailability from natural particles. *Environ. Sci. Technol.* **2013**, *47* (7), 3424−3431.
(30) Croteau, M. N.; Cain, D. J.; Fuller, C. C. Assessing the dietary bioavailability of metals associated with natural particles: extending the use of the reverse labeling approach to zinc. *Environ. Sci. Technol.* **2017**, *51* (5), 2803−2810.
(31) Xie, M.; Simpson, S. L.; Wang, W.-X. Bioturbation effects on metal release from contaminated sediments are metal-dependent. *Environ. Pollut.* **2019**, *250*, 87−96.
(32) Smith, M. E.; Lazorchak, J. M.; Herrin, L. E.; Brewer-Swartz, S.; Thoeny, W. T. A reformulated, reconstituted water for testing the freshwater amphipod, Hyalella azteca. *Environ. Toxicol. Chem.* **1997**, *16* (6), 1229−1233.
(33) Zhang, H.; Davison, W.; Mortimer, R. J.; Krom, M. D.; Hayes, P. J.; Davies, I. M. Localised remobilization of metals in a marine sediment. *Sci. Total Environ.* **2002**, *296* (1), 175−187.
(34) Harper, M. P.; Davison, W.; Zhang, H.; Tych, W. Kinetics of metal exchange between solids and solutions in sediments and soils interpreted from DGT measured fluxes. *Geochim. Cosmochim. Acta* **1998**, *62* (16), 2757−2770.
(35) Davison, W.; Zhang, H. In situ speciation measurements of trace components in natural waters using thin-film gels. *Nature* **1994**, *367* (6463), 546−548.
(36) Sarazin, G.; Michard, G.; Prevot, F. A rapid and accurate spectroscopic method for alkalinity measurements in sea water samples. *Water Res.* **1999**, *33* (1), 290−294.
(37) Allen, H.; Fu, G.; Boothman, W.; Di Toro, D.; Mahony, J. *Determination of Acid Volatile Sulfide and Selected Simultaneously Extractable Metals in Sediment; Office of Water Regulations and Standards*; US Environmental Protection Agency: Washington, DC, 1991; pp 1−22.
(38) Burton, E. D.; Bush, R. T.; Sullivan, L. A.; Hocking, R. K.; Mitchell, D. R.; Johnston, S. G.; Fitzpatrick, R.; Raven, M.; McClure, S.; Jang, L. Iron-monosulfide oxidation in natural sediments: resolving microbially mediated S transformations using XANES, electron microscopy, and selective extractions. *Environ. Sci. Technol.* **2009**, *43* (9), 3128−3134.
(39) Liu, W.; Guangyuan, L.; Wang, W.-X. In situ high-resolution two-dimensional profiles of redox sensitive metal mobility in sediment-water interface and porewater from estuarine sediments. *Sci. Total Environ.* **2022**, *820*, 153034.
(40) Zanella, L. The Role of Sulfides in the Speciation of Nickel in Anoxic Sediments. Doctor Of Philosophy, Northwestern University, Evanston, IL, 2011.
(41) Wang, W.; Wang, W.-X. Trace metal behavior in sediments of Jiulong River Estuary and implication for benthic exchange fluxes. *Environ. Pollut.* **2017**, *225*, 598−609.
(42) Qian, J.; Hu, T.; Xiong, H.; Cao, X.; Liu, F.; Gosnell, K. J.; Xie, M.; Chen, R.; Tan, Q.-G. Turbid Waters and Clearer Standards: Refining Water Quality Criteria for Coastal Environments by Encompassing Metal Bioavailability from Suspended Particles. *Environ. Sci. Technol.* **2024**, *58* (12), 5244−5254.
(43) Bloesch, J. Mechanisms, measurement and importance of sediment resuspension in lakes. *Mar. Freshw. Res.* **1995**, *46* (1), 295−304.
(44) Simpson, S.; Batley, G.; Chariton, A. Revision of the ANZECC/ARMCANZ sediment quality guidelines. *CSIRO Land and Water Report*, 2013; Vol. *8*, p 128.
(45) Simpson, S.; Batley, G. *Sediment Quality Assessment: A Practical Guide*; CSIRO Publishing: Melbourne, Victoria, Australia, 2016.
(46) Xie, M.; Simpson, S. L.; Huang, J.; Teasdale, P. R.; Wang, W.-X. In Situ DGT sensing of bioavailable metal fluxes to improve toxicity predictions for sediments. *Environ. Sci. Technol.* **2021**, *55* (11), 7355−7364.

https://doi.org/10.1021/acs.est.4c08327
Environ. Sci. Technol. XXXX, XXX, XXX−XXX